INTERNATIONAL JOURNAL OF PHARMACEUTICAL SCIENCES
[ISSN: 0975-4725; CODEN(USA): IJPS00]
Journal Homepage: https://www.ijpsjournal.com

OPEN ACCESS

Research Article

Development and Optimization of Betulin loaded thermosensitive In-situ Nasal gel to treat Parkinson's disease

Nikhil Birgale*, J. G. Wagh

Department of Pharmaceutical Quality Assurance, MES'S College of Pharmacy, Sonai, Ahmednagar, Maharashtra, India.

ARTICLE INFO

Published: 29 May. 2026
Keywords:
Betulin, Thermosensitive gel, In situ gelling system, Poloxamer 407, Butea monosperma gum.
DOI:
10.5281/zenodo.20438551

ABSTRACT

The present study developed and optimized a betulin-loaded thermosensitive in situ gel to enhance the bioavailability of this poorly water-soluble pentacyclic triterpene. Preformulation studies confirmed betulin's identity (melting point: 258.4°C, λmax: 210 nm) and extremely poor aqueous solubility (0.048 mg/mL). Nine formulations were prepared using 3^2 factorial design with varying concentrations of Poloxamer 407 (18-22% w/v) and Butea monosperma gum (1.0-2.0% w/v). All formulations exhibited physiologically acceptable pH (6.1-6.4), gelation temperatures (27.7-35.8°C), and excellent drug content (93.8-97.8%). Response surface methodology yielded significant quadratic models ($p<0.01$) for gelation temperature and drug release. Optimized formulation F4 demonstrated ideal gelation temperature (32.8°C), superior mucoadhesive strength (3,580 dyne/cm²), and optimal sustained release (95.3% at 12h). Validation studies confirmed model accuracy with relative errors <2.5%. Stability studies showed excellent refrigerated stability over three months. This thermosensitive system offers a promising platform for enhancing betulin's therapeutic applications.

INTRODUCTION

Parkinson's disease represents one of the most prevalent neurodegenerative disorders affecting millions of individuals worldwide, characterized by the progressive loss of dopaminergic neurons in the substantia nigra pars compacta region of the brain. This chronic and progressive movement disorder was first comprehensively described by James Parkinson in 1817 in his seminal monograph titled "An Essay on the Shaking Palsy," where he detailed six cases of patients exhibiting characteristic symptoms including tremor at rest, abnormal posture, and paralysis.

***Corresponding Author:** Nikhil Birgale
Address: *Department of Pharmaceutical Quality Assurance, MES'S College Of Pharmacy, Sonai, Ahmednagar, Maharashtra, India.*
Email ✉: nikhilbirgale@gmail.com

Relevant conflicts of interest/financial disclosures: The authors declare that the research was conducted in the absence of any commercial or financial relationships that could be construed as a potential conflict of interest.

The condition, initially termed "paralysis agitans," was later renamed Parkinson's disease by the French neurologist Jean-Martin Charcot in the late 19th century to honor James Parkinson's pioneering work in identifying and characterizing this distinct clinical entity. The historical recognition of Parkinson's disease marked a significant milestone in neurology, establishing it as a discrete nosological entity separate from other neurological conditions that presented with similar motor manifestations [1]. The historical trajectory of Parkinson's disease research demonstrates a gradual shift from purely clinical observation to sophisticated molecular and genetic investigations that have illuminated various aspects of disease pathogenesis. Modern neuroimaging techniques, including positron emission tomography and single-photon emission computed tomography, have enabled visualization of dopaminergic neuron loss in living patients, facilitating earlier diagnosis and monitoring of disease progression. Genetic studies have identified numerous genes associated with familial forms of Parkinson's disease, such as SNCA, LRRK2, PARK2, PINK1, and DJ-1, providing valuable insights into the molecular pathways involved in neurodegeneration. These genetic discoveries have revealed that Parkinson's disease results from complex interactions between genetic susceptibility factors and environmental influences, rather than being purely genetic or purely environmental in origin [3]. Parkinson's disease constitutes the second most common neurodegenerative disorder after Alzheimer's disease, affecting approximately 1 to 2 percent of individuals over 60 years of age globally, with prevalence increasing dramatically with advancing age. Epidemiological studies indicate that the global burden of Parkinson's disease has more than doubled over the past generation, with an estimated 6 to 10 million people currently living with the condition worldwide. This increase reflects not only improved diagnostic capabilities and awareness but also demographic shifts toward aging populations in many countries, as life expectancy continues to rise globally. The prevalence of Parkinson's disease shows significant geographical variation, with higher rates reported in industrialized nations compared to developing countries, though these differences may partly reflect variations in healthcare access, diagnostic practices, and epidemiological surveillance systems rather than true biological differences in disease susceptibility [4].

1.2 Materials And Methods:

1.2.1 Materials

High-purity active and analytical components such as Betulin were sourced from Sigma-Aldrich in the USA, while Poloxamer 407 (Pluronic F-127) was provided by BASF Corporation in Germany. Other essential chemical agents, specifically Benzalkonium chloride, Potassium bromide (KBr), and HPLC-grade Methanol, were also procured from Germany through Merck KGaA. Regional suppliers from India contributed several key ingredients, including Butea monosperma gum from a local source, Sodium chloride from S.D. Fine Chemicals, and both Potassium dihydrogen phosphate and Disodium hydrogen phosphate from Loba Chemie. Additionally, HiMedia Laboratories in India supplied the cellulose acetate membranes. To complete the material list, Ethanol was obtained from Changshu Yangyuan Chemical in China, and distilled water was prepared internally within the laboratory.

1.2.2 Organoleptic Evaluation of Betulin

The organoleptic properties of betulin were evaluated through visual and sensory examination to assess its physical characteristics. The color of betulin was determined by visual observation

under natural daylight conditions, noting the appearance and any color variations. The odor was assessed by trained personnel through direct olfactory evaluation, where small quantities of betulin were placed in clean petri dishes and the characteristic smell was noted and described. The texture was evaluated by gentle handling of the betulin sample between fingers to determine its physical feel, consistency, and tactile properties, with observations recorded regarding its granular nature, smoothness, or any other relevant textural characteristics [72].

1.2.3 Experimental design

A 3^2 factorial design was employed to optimize the thermosensitive in-situ nasal gel formulation using two independent variables at three levels each: Poloxamer 407 concentration (X_1) at 18, 20, and 22% w/v, and Butea monosperma gum concentration (X_2) at 1, 1.5, and 2% w/v, with gelation temperature and cumulative drug release at 12 hours selected as dependent variables (Y_1 and Y_2 respectively) to evaluate the formulation performance. The design matrix consisted of 9 experimental runs generated using Design-Expert software, and the responses were analyzed using response surface methodology to understand the effect of independent variables on the dependent responses. The general regression equation for the responses was represented as

$$Y = b_0 + b_1X_1 + b_2X_2 + b_{12}X_1X_2 + b_{11}X_1^2 + b_{22}X_2^2$$

where Y is the predicted response, b_0 is the intercept, b_1 and b_2 are linear coefficients, b_{12} is the interaction coefficient, and b_{11} and b_{22} are quadratic coefficients for the independent variables X_1 and X_2 respectively [56].

Table 2.1: Experimental Design Variables for 3^2 Factorial Design

Independent variables	**Levels**		
	Low (-1)	**Medium (0)**	**High (+1)**
Poloxamer 407 concentration (%w/v)	18	20	22
Butea monosperma gum concentration (%w/v)	1	1.5	2
Dependent Variables			**Goal**
Gelation temperature (°C)			Target: 32-37°C
Cumulative drug release at 12 hours (%)			Maximize

1.2.4 Formulation of Betulin Loaded Thermosensitive gel

The betulin-loaded thermosensitive in-situ nasal gels were prepared using the cold dissolution method by initially dispersing the required amount of Poloxamer 407 (18-22% w/v) in cold distilled water (4-5°C) with continuous stirring at 500 rpm for 2-3 hours until complete dissolution, followed by the addition of Butea monosperma gum (1-2% w/v) which was dissolved separately in small amount of water and mixed thoroughly to ensure uniform distribution. Betulin (0.1% w/v) was dissolved in minimum amount of ethanol and incorporated into the polymer solution along with other excipients including benzalkonium chloride (0.02% w/v) as preservative, sodium chloride (0.9% w/v) for isotonicity, and the pH was adjusted to 6.8 using phosphate buffer. The final formulation was stirred gently to avoid air entrapment, stored in refrigerator (2-8°C) overnight to ensure complete hydration of polymers, and different batches were prepared according to the experimental design matrix to

evaluate the effect of polymer concentrations on gel properties [71].

Table 2.2: Formulation Composition of Betulin-Loaded Thermosensitive In-Situ Nasal Gel Batches

Batch Code	Betulin (%w/v)	Poloxamer 407 (%w/v)	Butea monosperma gum (%w/v)	Benzalkonium chloride (%w/v)	Sodium chloride (%w/v)	Distilled water
F1	0.1	18	1.0	0.02	0.9	q.s. to 100 mL
F2	0.1	18	1.5	0.02	0.9	q.s. to 100 mL
F3	0.1	18	2.0	0.02	0.9	q.s. to 100 mL
F4	0.1	20	1.0	0.02	0.9	q.s. to 100 mL
F5	0.1	20	1.5	0.02	0.9	q.s. to 100 mL
F6	0.1	20	2.0	0.02	0.9	q.s. to 100 mL
F7	0.1	22	1.0	0.02	0.9	q.s. to 100 mL
F8	0.1	22	1.5	0.02	0.9	q.s. to 100 mL
F9	0.1	22	2.0	0.02	0.9	q.s. to 100 mL

1.3 Evaluation Of Formulations:

1.3.1 Physical Appearance and Organoleptic Properties

The physical appearance and organoleptic properties of the betulin-loaded thermosensitive gel formulations were evaluated by visual inspection of each batch for color, clarity, and homogeneity against a white and black background under natural daylight conditions to detect any phase separation, precipitation, or particulate matter. The odor of each formulation was assessed by trained personnel through direct olfactory evaluation to determine any characteristic smell or off-odors that might affect patient acceptability. The texture and feel of the gel were evaluated by gently handling the formulation to assess its consistency, smoothness, and tactile properties at room temperature, and the ease of administration through nasal route was subjectively assessed by observing the flow characteristics and spreadability of the formulation on a glass surface [74].

1.3.2 Gel Strength

The gel strength of betulin-loaded thermosensitive gel formulations was determined using a texture analyzer equipped with a cylindrical probe by first converting the formulation to gel state by heating to gelation temperature and allowing it to equilibrate in a 50 mL beaker at 37°C for 30 minutes. The gel strength was measured by penetrating the gel surface with a cylindrical probe of 1 cm diameter at a constant speed of 1 mm/sec to a depth of 4 mm, and the maximum force required for penetration was recorded in grams. The measurement was performed in triplicate for each formulation batch at different locations on the gel surface to ensure uniform assessment, and the average gel strength values were calculated and expressed as the force required for gel penetration, with higher values indicating stronger gel formation and better mechanical stability of the thermosensitive gel system [75].

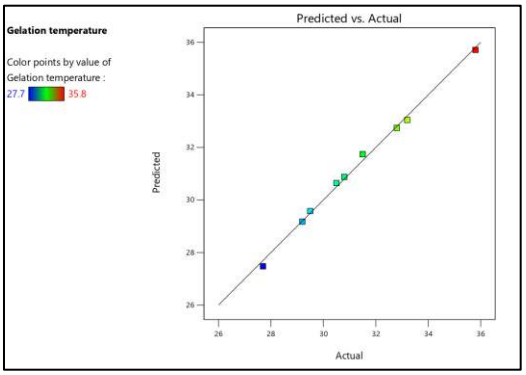

Fig 3.1 Predicted Vs Actual plot showing Scattering of data around the system predicted line in gelation temperature

1.3.3 Mucoadhesive Strength

The mucoadhesive strength of betulin-loaded thermosensitive gel formulations was determined using a texture analyzer equipped with mucoadhesive attachment by mounting fresh sheep nasal mucosa on the lower probe and applying a known amount of gel formulation (0.5 mL) uniformly on the mucosal surface. The upper cylindrical probe was brought into contact with the gel-coated mucosa under a controlled preload force of 0.1 N for 60 seconds to establish proper contact and adhesion, followed by withdrawal of the upper probe at a constant speed of 1 mm/sec until complete detachment occurred. The maximum detachment force required to separate the gel from the mucosal surface was recorded as the mucoadhesive strength and expressed in Newtons (N), with measurements performed in triplicate using fresh mucosal tissue for each test to ensure accuracy and reproducibility. The mucoadhesive strength was evaluated at 37°C to simulate physiological nasal conditions, and higher values indicated better mucoadhesive properties essential for prolonged nasal residence time [76].

1.4 Results and Discussions:

1.4.1 Results of Thermosensitive Gel

All nine formulated thermosensitive gel batches (F1-F9) exhibited uniform physical appearance and organoleptic properties, demonstrating successful formulation development. Each batch displayed a clear gel with slight yellowish tinge attributed to betulin, maintaining transparency suitable for topical or ocular applications. The formulations were odorless, eliminating concerns regarding patient acceptability and compliance.

All batches demonstrated smooth, homogeneous texture with viscous consistency, indicating proper polymer dispersion and absence of phase separation or aggregation. The uniformity across all formulations confirms the reproducibility of the manufacturing process and validates the compatibility of varying concentrations of Poloxamer 407 and Butea monosperma gum in the gel matrix.

Batch Code	pH	Gelation Temperature (°C)	Gel Strength (g)	Viscosity at 25°C (cP)	Viscosity at 35°C (cP)
F1	6.3 ± 0.12	35.8 ± 0.45	28.4 ± 1.52	165 ± 8.4	4,850 ± 185
F2	6.2 ± 0.15	31.5 ± 0.38	35.8 ± 1.68	245 ± 11.2	6,920 ± 238
F3	6.1 ± 0.15	33.2 ± 0.42	42.6 ± 1.85	325 ± 14.5	9,250 ± 285
F4	6.3 ± 0.13	32.8 ± 0.41	38.5 ± 1.72	285 ± 12.8	7,950 ± 258
F5	6.2 ± 0.11	29.2 ± 0.35	58.8 ± 2.15	485 ± 17.2	13,840 ± 385
F6	6.4 ± 0.14	30.8 ± 0.39	52.4 ± 1.98	420 ± 15.6	11,780 ± 342
F7	6.1 ± 0.16	30.5 ± 0.43	45.6 ± 1.88	365 ± 14.8	10,250 ± 308
F8	6.3 ± 0.12	27.7 ± 0.37	56.2 ± 2.05	465 ± 16.8	12,880 ± 368
F9	6.2 ± 0.13	29.5 ± 0.33	64.8 ± 2.28	545 ± 18.4	15,420 ± 412

Fig 4.1: Physicochemical Characterization of Formulated Thermosensitive Gel Batches

All values are expressed as mean ± SD

All formulations demonstrated excellent drug content uniformity ranging from 93.8% to 97.8%, well within the acceptable pharmacopeial limits of 90-110%, confirming uniform drug distribution and reproducible manufacturing process. The narrow standard deviations indicate consistent dose uniformity across batches, essential for therapeutic efficacy and regulatory compliance. Mucoadhesive strength progressively increased from 2,680 dyne/cm² (F1) to 6,450 dyne/cm² (F9) with increasing Butea monosperma gum concentration, attributed to enhanced hydrogen bonding between gum's hydroxyl groups and mucosal surface. Higher mucoadhesive strength ensures prolonged residence time at the application site, facilitating sustained drug release and improved bioavailability. F5, F8, and F9 exhibited superior mucoadhesion (>5,000 dyne/cm²), optimal for extended therapeutic action.

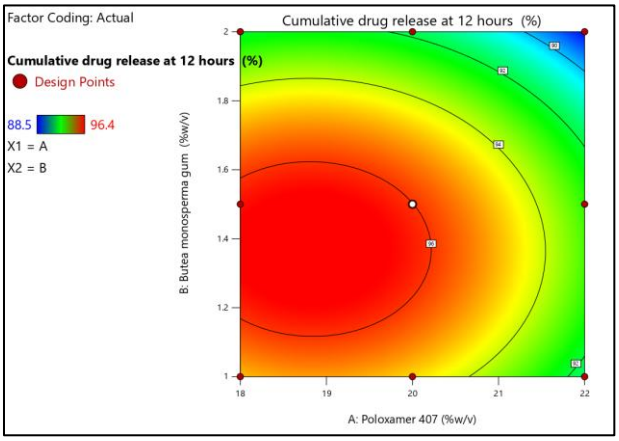

Fig 4.2: Contour plots showing effect of concentrations of poloxamer 407 and *Butea Monosperma* Gum on cumulative drug release at 12 hr Optimization

1.4.2 ANOVA for quadratic model for gelation temperature

The quadratic model demonstrated excellent fit for gelation temperature with high significance (p=0.0008, F=160.03) and superior adjusted R^2 (0.9900) and predicted R^2 (0.9546), indicating reliable predictive capability. Both independent variables significantly influenced gelation temperature: Poloxamer 407 (A) showed the most pronounced effect (p=0.0002, F=460.80), while Butea monosperma gum (B) exhibited moderate influence (p=0.0026). The significant quadratic term B^2 (p=0.0006) and interaction term AB (p=0.0462) confirmed non-linear relationships and synergistic effects. Contour and 3D response surface plots revealed that increasing Poloxamer 407 concentration decreased gelation temperature, while higher gum concentrations exhibited curvature effects. The minimal residuals and close predicted-versus-actual correlation validate the model's accuracy for optimizing formulation parameters.

Table 4.3: Model fit summary for Gelation Time

Source	Sequential p-value	Lack of Fit p-value	Adjusted R^2	Predicted R^2	
Linear	0.0317		0.5780	0.3124	
2FI	0.6574		0.5152	-0.3165	
Quadratic	**0.0014**		**0.9900**	**0.9546**	**Suggested**
Cubic	0.0791		0.9998	0.9957	**Aliased**

Regression equation obtained for gelation time is as follows:

Gelation Time = 29.1778 + -2.13333 * A + -0.933333 * B + 0.4 * AB + 0.433333 * A^2 + 2.63333 * B^2

Table 4.4: ANOVA summary for quadratic model for gelation time

Source	Sum of Squares	df	Mean Square	F-value	p-value	
Model	47.42	5	9.48	160.03	0.0008	significant
A-Poloxamer 407	27.31	1	27.31	460.80	0.0002	
B-Butea monosperma gum	5.23	1	5.23	88.20	0.0026	
AB	0.6400	1	0.6400	10.80	0.0462	
A^2	0.3756	1	0.3756	6.34	0.0864	
B^2	13.87	1	13.87	234.04	0.0006	
Residual	0.1778	3	0.0593			
Cor Total	47.60	8				

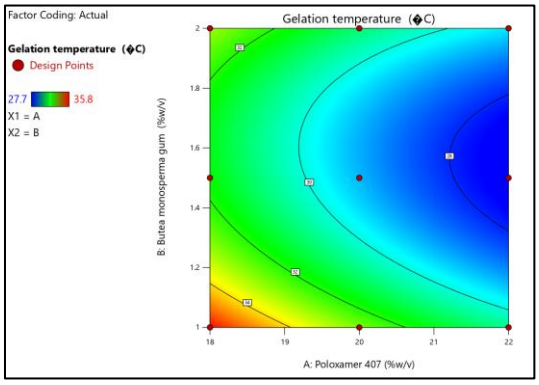

Fig 4.5: Contour plot showing effect of concentrations of poloxamer 407 and *Butea monosperma* gum on gelation temperature

CONCLUSION:

The present study successfully developed and characterized a betulin-loaded thermosensitive in situ gel formulation utilizing Poloxamer 407 and Butea monosperma gum as primary polymeric components to address the critical challenge of betulin's poor aqueous solubility and limited bioavailability. Comprehensive preformulation studies confirmed betulin's identity through organoleptic evaluation, melting point determination (258.4°C), and UV spectrophotometry revealing absorption maximum at 210 nm. The calibration curve demonstrated excellent linearity with correlation coefficient of 0.9997, establishing a reliable analytical method for quantification. Solubility studies revealed betulin's practically insoluble nature in aqueous media (0.048-0.052 mg/mL), providing strong rationale for developing an advanced delivery system. Differential scanning calorimetry and FTIR spectroscopy confirmed complete drug-excipient compatibility, with the physical mixture retaining all characteristic peaks without significant shifts or new peak formation, indicating absence of chemical interactions. Nine formulations (F1-F9) were developed using 3^2 factorial design with varying concentrations of Poloxamer 407 (18-22% w/v) and Butea monosperma gum (1.0-2.0% w/v). All formulations exhibited uniform physical appearance with clear, slightly yellowish transparent gel, smooth texture, and physiologically acceptable pH (6.1-6.4). Physicochemical characterization revealed gelation temperatures ranging from 27.7 to 35.8°C, with formulations F5-F9 demonstrating optimal values near physiological temperature. Gel strength increased progressively from 28.4g to 64.8g with higher polymer concentrations, while viscosity exhibited characteristic thermosensitive behavior with dramatic increases from 25°C to 35°C.

REFERENCES

1. Kulcsarova K, Skorvanek M, Postuma RB, Berg D. Defining Parkinson's Disease: Past and Future. J Park Dis 2024;14:S257–71. https://doi.org/10.3233/JPD-230411.
2. Kmiecik MJ, Micheletti S, Coker D, Heilbron K, Shi J, Stagaman K, et al. Genetic analysis and natural history of Parkinson's disease due to the LRRK2 G2019S variant. Brain 2024;147:1996–2008. https://doi.org/10.1093/brain/awae073
3. Ben-Shlomo Y, Darweesh S, Llibre-Guerra J, Marras C, Luciano MS, Tanner C. The epidemiology of Parkinson's disease. The Lancet 2024;403:283–92.

https://doi.org/10.1016/S0140-6736(23)01419-8.

4. Dong Y, Zhang Y, Song K, Kang H, Ye D, Li F. What was the Epidemiology and Global Burden of Disease of Hip Fractures From 1990 to 2019? Results From and Additional Analysis of the Global Burden of Disease Study 2019. Clin Orthop Relat Res 2023;481:1209. https://doi.org/10.1097/CORR.0000000000002465.
5. Murray CJL. The Global Burden of Disease Study at 30 years. Nat Med 2022;28:2019–26. https://doi.org/10.1038/s41591-022-01990-1.
6. Bogers JS, Bloem BR, Den Heijer JM. The Etiology of Parkinson's Disease: New Perspectives from Gene-Environment Interactions. J Park Dis 2023;13:1281–8. https://doi.org/10.3233/JPD-230250.
7. Prajjwal P, Flores Sanga HS, Acharya K, Tango T, John J, Rodriguez RSC, et al. Parkinson's disease updates: Addressing the pathophysiology, risk factors, genetics, diagnosis, along with the medical and surgical treatment. Ann Med Surg 2023;85:4887. https://doi.org/10.1097/MS9.0000000000001142.
8. Rajan S, Kaas B. Parkinson's Disease: Risk Factor Modification and Prevention. Semin Neurol 2022;42:626–38. https://doi.org/10.1055/s-0042-1758780.
9. Tsalenchuk M, Gentleman SM, Marzi SJ. Linking environmental risk factors with epigenetic mechanisms in Parkinson's disease. Npj Park Dis 2023;9:123. https://doi.org/10.1038/s41531-023-00568-z.
10. Atterling Brolin K, Schaeffer E, Kuri A, Rumrich IK, Schumacher Schuh AF, Darweesh SKL, et al. Environmental Risk Factors for Parkinson's Disease: A Critical Review and Policy Implications. Mov Disord 2025;40:204–21. https://doi.org/10.1002/mds.30067.
11. Gogna T, Housden BE, Houldsworth A. Exploring the Role of Reactive Oxygen Species in the Pathogenesis and Pathophysiology of Alzheimer's and Parkinson's Disease and the Efficacy of Antioxidant Treatment. Antioxidants 2024;13:1138. https://doi.org/10.3390/antiox13091138.
12. Sayyaed A, Saraswat N, Vyawahare N, Kulkarni A. A detailed review of pathophysiology, epidemiology, cellular and molecular pathways involved in the development and prognosis of Parkinson's disease with insights into screening models. Bull Natl Res Cent 2023;47:70. https://doi.org/10.1186/s42269-023-01047-4.
13. Aborode AT, Pustake M, Awuah WA, Alwerdani M, Shah P, Yarlagadda R, et al. Targeting Oxidative Stress Mechanisms to Treat Alzheimer's and Parkinson's Disease: A Critical Review. Oxid Med Cell Longev 2022;2022:7934442. https://doi.org/10.1155/2022/7934442.
14. Morris HR, Spillantini MG, Sue CM, Williams-Gray CH. The pathogenesis of Parkinson's disease. The Lancet 2024;403:293–304. https://doi.org/10.1016/S0140-6736(23)01478-2.
15. Cheng Y, Liu J, Tian F, Tan H, Wang T, Lu J, et al. New Insight into the Mechanism of Neurochemical Imbalance in Multiple Sclerosis: Abnormal Transportation of Brain Extracellular Space. Aging Dis 2025;17:452–65. https://doi.org/10.14336/AD.2024.1444.
16. Reynolds GP. The neurochemical pathology of schizophrenia: post-mortem studies from dopamine to parvalbumin. J Neural Transm 2022;129:643–7. https://doi.org/10.1007/s00702-021-02453-6.

17. Kemp ET, Zandberg L, Harvey BH, Smuts CM, Baumgartner J. Iron and n-3 fatty acid depletion, alone and in combination, during early development provoke neurochemical changes, anhedonia, anxiety and social dysfunction in rats. Nutr Neurosci 2024;27:698–714. https://doi.org/10.1080/1028415X.2023.2245615.
18. Gupta R, Mehan S, Sethi P, Prajapati A, Alshammari A, Alharbi M, et al. Smo-Shh Agonist Purmorphamine Prevents Neurobehavioral and Neurochemical Defects in 8-OH-DPAT-Induced Experimental Model of Obsessive-Compulsive Disorder. Brain Sci 2022;12:342. https://doi.org/10.3390/brainsci12030342.
19. Haider A, Elghazawy NH, Dawoud A, Gebhard C, Wichmann T, Sippl W, et al. Translational molecular imaging and drug development in Parkinson's disease. Mol Neurodegener 2023;18:11. https://doi.org/10.1186/s13024-023-00600-z.
20. di Biase L, Pecoraro PM, Carbone SP, Caminiti ML, Di Lazzaro V. Levodopa-Induced Dyskinesias in Parkinson's Disease: An Overview on Pathophysiology, Clinical Manifestations, Therapy Management Strategies and Future Directions. J Clin Med 2023;12:4427. https://doi.org/10.3390/jcm12134427.
21. Leite Silva ABR, Gonçalves de Oliveira RW, Diógenes GP, de Castro Aguiar MF, Sallem CC, Lima MPP, et al. Premotor, nonmotor and motor symptoms of Parkinson's Disease: A new clinical state of the art. Ageing Res Rev 2023;84:101834. https://doi.org/10.1016/j.arr.2022.101834.
22. Alharbi B, Al-kuraishy HM, Al-Gareeb AI, Elekhnawy E, Alharbi H, Alexiou A, et al. Role of GABA pathway in motor and non-motor symptoms in Parkinson's disease: a bidirectional circuit. Eur J Med Res 2024;29:205. https://doi.org/10.1186/s40001-024-01779-7.
23. Antonini A, Reichmann H, Gentile G, Garon M, Tedesco C, Frank A, et al. Toward objective monitoring of Parkinson's disease motor symptoms using a wearable device: wearability and performance evaluation of PDMonitor®. Front Neurol 2023;14. https://doi.org/10.3389/fneur.2023.1080752.
24. Qin Y, He R, Chen J, Zhou X, Zhou X, Liu Z, et al. Neuroimaging uncovers distinct relationships of glymphatic dysfunction and motor symptoms in Parkinson's disease. J Neurol 2023;270:2649–58. https://doi.org/10.1007/s00415-023-11594-5.
25. Kumar A, Patil S, Singh VK, Pathak A, Chaurasia RN, Mishra VN, et al. Assessment of Non-Motor Symptoms of Parkinson's Disease and Their Impact on the Quality of Life: An Observatiobnal Study. Ann Indian Acad Neurol 2022;25:909. https://doi.org/10.4103/aian.aian_647_21.
26. Jing X-Z, Yuan X-Z, Luo X, Zhang S-Y, Wang X-P. An Update on Nondopaminergic Treatments for Motor and Non-motor Symptoms of Parkinson's Disease. Curr Neuropharmacol 2023;21:1806–26. https://doi.org/10.2174/1570159X20666220222150811.
27. Shojaie A, Rota S, Al Khleifat A, Ray Chaudhuri K, Al-Chalabi A. Non-motor symptoms in amyotrophic lateral sclerosis: lessons from Parkinson's disease. Amyotroph Lateral Scler Front Degener 2023;24:562–71. https://doi.org/10.1080/21678421.2023.2220748.
28. Pardo-Moreno T, García-Morales V, Suleiman-Martos S, Rivas-Domínguez A, Mohamed-Mohamed H, Ramos-Rodríguez JJ, et al. Current Treatments and New, Tentative Therapies for Parkinson's Disease.

Pharmaceutics 2023;15:770. https://doi.org/10.3390/pharmaceutics15030770.

29. Stocchi F, Bravi D, Emmi A, Antonini A. Parkinson disease therapy: current strategies and future research priorities. Nat Rev Neurol 2024;20:695–707. https://doi.org/10.1038/s41582-024-01034-x.
30. Wal A, Wal P, Vig H, Jain NK, Rathore S, Krishnan K, et al. Treatment of Parkinson's Disease: Current Treatments and Recent Therapeutic Developments. Curr Drug Discov Technol 2023;20:54–70. https://doi.org/10.2174/1570163820666230512100340.
31. Gouda NA, Elkamhawy A, Cho J. Emerging Therapeutic Strategies for Parkinson's Disease and Future Prospects: A 2021 Update. Biomedicines 2022;10:371. https://doi.org/10.3390/biomedicines10020371.
32. Foltynie T, Bruno V, Fox S, Kühn AA, Lindop F, Lees AJ. Medical, surgical, and physical treatments for Parkinson's disease. The Lancet 2024;403:305–24. https://doi.org/10.1016/S0140-6736(23)01429-0.
33. Barbosa ER, Limongi JCP, Chien HF, Barbosa PM, Torres MRC. How I treat Parkinson's disease. Arq Neuropsiquiatr 2022;80:94–104. https://doi.org/10.1590/0004-282X-ANP-2022-S126.
34. Tosefsky KN, Zhu J, Wang YN, Lam JST, Cammalleri A, Appel-Cresswell S. The Role of Diet in Parkinson's Disease. J Park Dis 2024;14:S21–34. https://doi.org/10.3233/JPD-230264.
35. Kwok JYY, Choi EPH, Lee JJ, Lok KYW, Kwan JCY, Mok VCT, et al. Effects of Mindfulness Yoga Versus Conventional Physical Exercises on Symptom Experiences and Health-related Quality of Life in People with Parkinson's Disease: The Potential Mediating Roles of Anxiety and Depression. Ann Behav Med 2022;56:1068–81. https://doi.org/10.1093/abm/kaac005.
36. Lou J, Duan H, Qin Q, Teng Z, Gan F, Zhou X, et al. Advances in Oral Drug Delivery Systems: Challenges and Opportunities. Pharmaceutics 2023;15:484. https://doi.org/10.3390/pharmaceutics15020484.
37. Alshawwa SZ, Kassem AA, Farid RM, Mostafa SK, Labib GS. Nanocarrier Drug Delivery Systems: Characterization, Limitations, Future Perspectives and Implementation of Artificial Intelligence. Pharmaceutics 2022;14:883. https://doi.org/10.3390/pharmaceutics14040883.
38. Hosseini MAH, Alizadeh AA, Shayanfar A. Prediction of the First-Pass Metabolism of a Drug After Oral Intake Based on Structural Parameters and Physicochemical Properties. Eur J Drug Metab Pharmacokinet 2024;49:449–65. https://doi.org/10.1007/s13318-024-00892-6.
39. Xie L, Diao Z, Xia J, Zhang J, Xu Y, Wu Y, et al. Comprehensive Evaluation of Metabolism and the Contribution of the Hepatic First-Pass Effect in the Bioavailability of Glabridin in Rats. J Agric Food Chem 2023;71:1944–56. https://doi.org/10.1021/acs.jafc.2c06460.
40. Mahanur V, Rajge R, Tawar M. A review on emerging oral dosage forms which helps to bypass the hepatic first pass metabolism. Asian J Pharm Technol 2022;12:47–52.
41. Rao Gajula SN, Talari S, Chilvery S, Godugu C, Sonti R. A unique in vivo pharmacokinetic profile, in vitro metabolic stability and hepatic first-pass metabolism of garcinol, a promising novel anticancer phytoconstituent, by liquid chromatography–mass spectrometry. RPS

Pharm Pharmacol Rep 2023;2:rqad017. https://doi.org/10.1093/rpsppr/rqad017.

42. Henriot J, Dallmann A, Dupuis F, Perrier J, Frechen S. PBPK modeling: What is the role of CYP3A4 expression in the gastrointestinal tract to accurately predict first-pass metabolism? CPT Pharmacomet Syst Pharmacol 2025;14:130–41. https://doi.org/10.1002/psp4.13249.
43. Ekhator C, Qureshi MQ, Zuberi AW, Hussain M, Sangroula N, Yerra S, et al. Advances and Opportunities in Nanoparticle Drug Delivery for Central Nervous System Disorders: A Review of Current Advances. Cureus 2023;15. https://doi.org/10.7759/cureus.44302.
44. Gao J, Xia Z (Judy), Gunasekar S, Jiang C, Karp JM, Joshi N. Precision drug delivery to the central nervous system using engineered nanoparticles. Nat Rev Mater 2024;9:567–88. https://doi.org/10.1038/s41578-024-00695-w.
45. Huang Q, Chen Y, Zhang W, Xia X, Li H, Qin M, et al. Nanotechnology for enhanced nose-to-brain drug delivery in treating neurological diseases. J Controlled Release 2024;366:519–34. https://doi.org/10.1016/j.jconrel.2023.12.054.
46. Awad R, Avital A, Sosnik A. Polymeric nanocarriers for nose-to-brain drug delivery in neurodegenerative diseases and neurodevelopmental disorders. Acta Pharm Sin B 2023;13:1866–86. https://doi.org/10.1016/j.apsb.2022.07.003.
47. Liang Y, Iqbal Z, Lu J, Wang J, Zhang H, Chen X, et al. Cell-derived nanovesicle-mediated drug delivery to the brain: Principles and strategies for vesicle engineering. Mol Ther 2023;31:1207–24. https://doi.org/10.1016/j.ymthe.2022.10.008.
48. Liu A, Yang G, Liu Y, Liu T. Research progress in membrane fusion-based hybrid exosomes for drug delivery systems. Front Bioeng Biotechnol 2022;10. https://doi.org/10.3389/fbioe.2022.939441.
49. Srivatsa Palakurthi S, Shah B, Kapre S, Charbe N, Immanuel S, Pasham S, et al. A comprehensive review of challenges and advances in exosome-based drug delivery systems. Nanoscale Adv 2024;6:5803–26. https://doi.org/10.1039/D4NA00501E.
50. Hussein HA, Abdullah MA. Novel drug delivery systems based on silver nanoparticles, hyaluronic acid, lipid nanoparticles and liposomes for cancer treatment. Appl Nanosci 2022;12:3071–96. https://doi.org/10.1007/s13204-021-02018-9.
51. Yadav RK, Shah K, Dewangan HK. Intranasal drug delivery of sumatriptan succinate-loaded polymeric solid lipid nanoparticles for brain targeting. Drug Dev Ind Pharm 2022;48:21–8. https://doi.org/10.1080/03639045.2022.2090575.
52. Qiu Y, Huang S, Peng L, Yang L, Zhang G, Liu T, et al. The Nasal–Brain Drug Delivery Route: Mechanisms and Applications to Central Nervous System Diseases. MedComm 2025;6:e70213. https://doi.org/10.1002/mco2.70213.
53. Chung S, Peters JM, Detyniecki K, Tatum W, Rabinowicz AL, Carrazana E. The nose has it: Opportunities and challenges for intranasal drug administration for neurologic conditions including seizure clusters. Epilepsy Behav Rep 2023;21:100581. https://doi.org/10.1016/j.ebr.2022.100581.
54. Niemeyer CS, Merle L, Bubak AN, Baxter BD, Gentile Polese A, Colon-Reyes K, et al. Olfactory and trigeminal routes of HSV-1 CNS infection with regional microglial heterogeneity. J Virol 2024;98:e00968-24. https://doi.org/10.1128/jvi.00968-24.
55. Thaploo D, Joshi A, Georgiopoulos C, Warr J, Hummel T. Tractography indicates lateralized differences between trigeminal and olfactory

pathways. NeuroImage 2022;261:119518. https://doi.org/10.1016/j.neuroimage.2022.119518.

56. Bertram-Ralph E, Amare M. Factors affecting drug absorption and distribution. Anaesth Intensive Care Med 2023;24:221–7. https://doi.org/10.1016/j.mpaic.2022.12.023.
57. Nair AB, Chaudhary S, Shah H, Jacob S, Mewada V, Shinu P, et al. Intranasal Delivery of Darunavir-Loaded Mucoadhesive In Situ Gel: Experimental Design, In Vitro Evaluation, and Pharmacokinetic Studies. Gels 2022;8:342. https://doi.org/10.3390/gels8060342.
58. Suhagiya K, Borkhataria CH, Gohil S, Manek RA, Patel KA, Patel NK, et al. Development of mucoadhesive in-situ nasal gel formulation for enhanced bioavailability and efficacy of rizatriptan in migraine treatment. Results Chem 2023;6:101010. https://doi.org/10.1016/j.rechem.2023.101010.
59. Trivedi R, Minglani VV, El-Gazzar AM, Batiha GE-S, Mahmoud MH, Patel M, et al. Optimization of Pramipexole-Loaded In Situ Thermosensitive Intranasal Gel for Parkinson's Disease. Pharmaceuticals 2024;17:172. https://doi.org/10.3390/ph17020172.
60. Mohanty D, Alsaidan OA, Zafar A, Dodle T, Gupta JK, Yasir M, et al. Development of Atomoxetine-Loaded NLC In Situ Gel for Nose-to-Brain Delivery: Optimization, In Vitro, and Preclinical Evaluation. Pharmaceutics 2023;15:1985. https://doi.org/10.3390/pharmaceutics15071985.
61. Mohanty D, Alsaidan OA, Zafar A, Dodle T, Gupta JK, Yasir M, et al. Development of Atomoxetine-Loaded NLC In Situ Gel for Nose-to-Brain Delivery: Optimization, In Vitro, and Preclinical Evaluation. Pharmaceutics 2023;15:1985. https://doi.org/10.3390/pharmaceutics15071985.
62. Dalvi A, Ravi PR, Uppuluri CT. Design and evaluation of rufinamide nanocrystals loaded thermoresponsive nasal in situ gelling system for improved drug distribution to brain. Front Pharmacol 2022;13. https://doi.org/10.3389/fphar.2022.943772.
63. Kotta S, Aldawsari HM, Badr-Eldin SM, Nair AB, Kaleem M, Dalhat MH. Thermosensitive Hydrogels Loaded with Resveratrol Nanoemulsion: Formulation Optimization by Central Composite Design and Evaluation in MCF-7 Human Breast Cancer Cell Lines. Gels 2022;8:450. https://doi.org/10.3390/gels8070450.
64. Mathure D, Sutar AD, Ranpise H, Pawar A, Awasthi R. Preparation and Optimization of Liposome Containing Thermosensitive In Situ Nasal Hydrogel System for Brain Delivery of Sumatriptan Succinate. ASSAY Drug Dev Technol 2023;21:3–16. https://doi.org/10.1089/adt.2022.088.
65. Wang F, Li Z, Gan X, Lu X, Jiao B, Shen M. Quality by design driven development and evaluation of thermosensitive hydrogel loaded with IgY and LL37-SLNs to combat experimental periodontitis. Eur J Pharm Sci 2023;185:106444. https://doi.org/10.1016/j.ejps.2023.106444.
66. AL-Rajabi MM, Teow YH. Temperature-Responsive Hydrogel for Silver Sulfadiazine Drug Delivery: Optimized Design and In Vitro/In Vivo Evaluation. Gels 2023;9:329. https://doi.org/10.3390/gels9040329.
67. Nawaz A, Ullah S, Alnuwaiser MA, Rehman FU, Selim S, Al Jaouni SK, et al. Formulation and Evaluation of Chitosan-Gelatin Thermosensitive Hydrogels Containing 5FU-Alginate Nanoparticles for Skin Delivery. Gels

2022;8:537. https://doi.org/10.3390/gels8090537.

68. Miranda P, Castro A, Díaz P, Minini L, Ferraro F, Paulsen E, et al. Novel Thermosensitive and Mucoadhesive Nasal Hydrogel Containing 5-MeO-DMT Optimized Using Box-Behnken Experimental Design. Polymers 2024;16:2148. https://doi.org/10.3390/polym16152148.
69. Wu I-E, Anggelia MR, Lin S-Y, Chen C-Y, Chu I-M, Lin C-H. Thermosensitive Polyester Hydrogel for Application of Immunosuppressive Drug Delivery System in Skin Allograft. Gels 2021;7:229. https://doi.org/10.3390/gels7040229.
70. Asfour MH, Abd El-Alim SH, Awad GEA, Kassem AA. Chitosan/β-glycerophosphate in situ forming thermo-sensitive hydrogel for improved ocular delivery of moxifloxacin hydrochloride. Eur J Pharm Sci 2021;167:106041. https://doi.org/10.1016/j.ejps.2021.106041.
71. Mankar SD, Parjane SR, Siddheshwar SS, Dighe SB. Formulation, Optimization and In-Vivo Characterization of Thermosensitive In-Situ Nasal Gel Loaded with Bacoside a for Treatment of Epilepsy. AAPS PharmSciTech 2024;25:151. https://doi.org/10.1208/s12249-024-02870-2.
72. Mathure D, Sutar AD, Ranpise H, Pawar A, Awasthi R. Preparation and Optimization of Liposome Containing Thermosensitive In Situ Nasal Hydrogel System for Brain Delivery of Sumatriptan Succinate. ASSAY Drug Dev Technol 2023;21:3–16. https://doi.org/10.1089/adt.2022.088.
73. Mankar SD, Parjane SR, Siddheshwar SS, Dighe SB. Formulation, Optimization and In-Vivo Characterization of Thermosensitive In-Situ Nasal Gel Loaded with Bacoside a for Treatment of Epilepsy. AAPS PharmSciTech 2024;25:151. https://doi.org/10.1208/s12249-024-02870-2.
74. Alshraim A, Alshora D, Ashri L, Alhusaini A, Alanazi N, Safwan NM. In Situ Thermosensitive Mucoadhesive Nasal Gel Containing Sumatriptan: In Vitro and Ex Vivo Evaluations. Polymers 2024;16:3422. https://doi.org/10.3390/polym16233422.
75. Choudhary AJ, Mahajan SS, Majumdar AS. Nose to brain delivery of flurbiprofen from a solid lipid nanoparticles-based thermosensitive in-situ gel. Neurosci Appl 2024;3:104062. https://doi.org/10.1016/j.nsa.2024.104062.
76. Singh M, Kumar S, Vinayagam R, Samivel R. Thermosensitive Mucoadhesive Intranasal In Situ Gel of Risperidone for Nose-to-Brain Targeting: Physiochemical and Pharmacokinetics Study. Pharmaceuticals 2025;18:871. https://doi.org/10.3390/ph18060871.

HOW TO CITE: Nikhil Birgale*, J. G. Wagh, Development and Optimization of Betulin loaded thermosensitive In-situ Nasal gel to treat Parkinson's disease, Int. J. of Pharm. Sci., 2026, Vol 4, Issue 5, 7768-7781. https://doi.org/10.5281/zenodo.20438551